Title: Local muscle pressure stimulates the principal receptors for proprioception

Frida Torell[1] & Michael Dimitriou[1,*]

[1] Department of Medical and Translational Biology, Umeå University, S-901 87, Umeå, Sweden

*Lead contact and corresponding author (michael.dimitriou@umu.se)

HIGHLIGHTS

1. Local muscle pressure is an adequate stimulus for spindles in isometric conditions
2. Local pressure enhances spindle afferent responses during muscle stretch
3. Spindles are better at encoding pressure in isometric conditions than kinematics during stretch

SUMMARY

Proprioception plays a vital role in motor coordination and self-perception. Muscle spindles are considered the principal receptors for proprioception and are believed to encode stretch and signal limb position and velocity. Here, we applied percutaneous pressure on a small area of extensor muscles at the forearm while simultaneously recording spindle afferent responses, skeletal muscle activity and hand kinematics. Three target levels of press force were applied periodically on the spindle-bearing muscle when the hand was immobile ('isometric' condition) and when the participant's hand moved rhythmically about the wrist in the flexion-extension plane ('sinusoidal' condition). We show that local muscle pressure is an 'adequate' stimulus for human spindles in isometric conditions, and that pressure enhances spindle afferent responses during stretch, as hypothesized to occur due to compression of the spindle capsule. Our findings redefine basic muscle feedback and urge a reconsideration of its role in sensorimotor function and various neuromuscular pathologies.

KEYWORDS: proprioception, muscle spindle, afferent, muscle pressure, intramuscular pressure, somatosensory

INTRODUCTION

It is well established that intramuscular fluid pressure (IMP) increases with contractile force and passive muscle elongation[1-3]. IMP has proven a better index of muscle force than muscle electrical activity (Electromyography: EMG), especially so in the case of eccentric contractions, muscle fatigue and recovery[4,5]. It is also known that single motor unit activity involves sharp increases in pressure within the motor unit territory, with no effect at more distant sites in the muscle, and that IMP influences the degree of actively produced muscle force[6]. It follows that access to sensory feedback concerning muscle pressure gradients would empower more robust sensorimotor function, such as by directly incorporating the muscle's fluidic behavior in segmental reflex arcs and more global muscle activation strategies[7]. However, with regard to skeletal muscle proprioception, it is generally believed that the nervous system receives major sensory feedback only about stretch and global tension via muscle spindles and Golgi tendon organs, respectively (e.g., [8,9]).

Muscle spindles are considered the principal receptors for proprioception[8,10]. Spindles can encode muscle stretch[11] and their afferent signals have been implicated in a variety of sensorimotor functions including reflex control and the update of internal models of limb dynamics[12,13]. Recent studies have suggested additional functions for proprioceptive feedback, including in the maintenance of spinal realignment[14] and the proper healing of fractured bones[15]. Moreover, in the early 1960's, Bridgman and Eldred put forward a hypothesis that

the secondary ending of the muscle spindle organ may be able to function as a pressure-sensing mechanism[16]. Specifically, they argued that pressure acting on the expanded equatorial area of the spindle organ will compress and elongate the fluid-filled capsule, stretching the intrafusal fibers terminating inside the capsule (the more numerous "nuclear chain" fibers[17,18]), and stimulating the spindle receptor ending. However, there has been no systematic investigation of the ability of spindles to encode locally applied muscle pressure. Here, we assess an updated version of the original hypothesis: whether primary and secondary spindle receptors of awake humans can encode local muscle pressure (i.e., both endings engage nuclear chain fibers[19]).

Specifically, in this study, we applied pressure percutaneously on one of three major extensor muscles of the forearm using a hand-held probe (5mm tip diameter) while recoding spindle afferent activity from this muscle, as well as monitoring skeletal muscle activity (EMG) and hand kinematics (Figure 1A). Three target levels of press force were sequentially applied when the hand was immobile ('isometric' condition) and when the participant's hand was moved rhythmically about the wrist by the experimenter in the flexion-extension dimension at a 0.5 Hz pace ('sinusoidal' condition; Figure 1B). We also present three spindle afferent recordings where the participants performed sinusoidal movements actively, with and without the muscle press stimulus, for comparison.

RESULTS

The left panel of Figure 1C displays the responses of an exemplary spindle afferent recorded during the 'isometric' condition. There is vigorous afferent firing in response to locally applied pressure on the spindle-bearing muscle. The right panel of Figure 1C shows that the same afferent responds with higher firing rates during wrist flexion (i.e., muscle stretch) when pressure is applied.

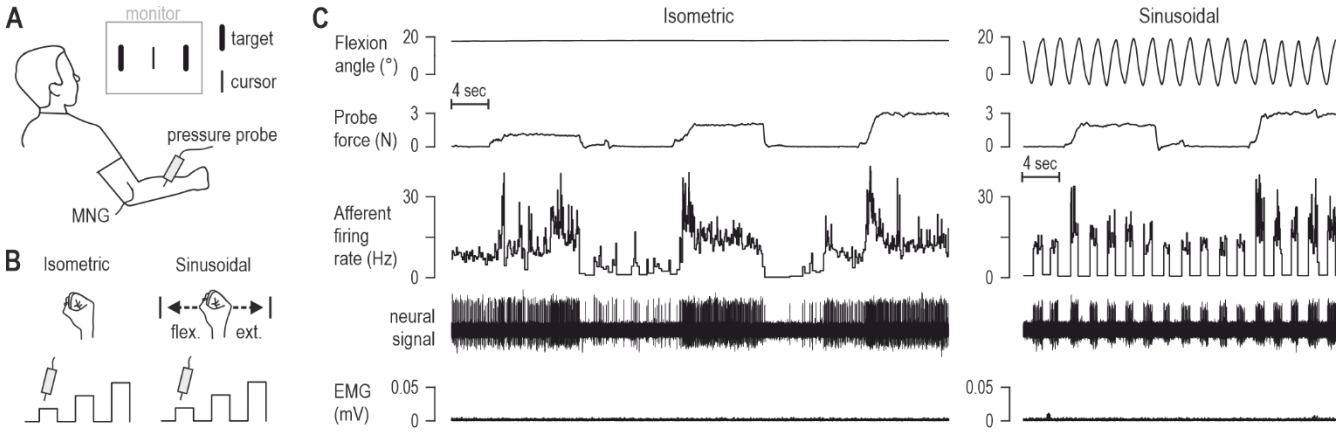

Figure 1. Experimental set-up and exemplary spindle afferent responses.

A) Microneurography (MNG) was used for recording from muscle spindle afferents (n=14) in the right radial nerve of 8 awake individuals, while a probe applied pressure on a small part of the forearm (circular tip, 5mm diameter; see Methods section for more details). A kinematic sensor attached to the dorsum of the participant's hand tracked movement about the wrist in the flexion-extension dimension. Surface EMG electrodes recorded muscle activity of wrist and finger extensor muscles from which the recorded spindle afferents originated. A monitor displayed two immobile visual targets and a cursor that tracked hand movement. **B)** The experimental task involved two conditions. In the first condition ('isometric'), the semi-pronated hand was immobile whereas in the 'sinusoidal' condition the experimenter moved the participant's hand continuously in the flexion-extension dimension so that the cursor reached the visual targets at a 0.5 Hz pace. In both conditions, three target levels of press force (1 - 3N) were sequentially applied at 10 sec intervals, at the location on the forearm where the spindle afferent was most responsive to brief taps. Three of the participants also performed sinusoidal movements actively, for comparison of spindle behavior. **C)** Left: raw data of a spindle afferent from the extensor carpi radialis muscle during the isometric condition. Right: data from the same afferent/participant during the latter parts of the sinusoidal condition.

Local muscle pressure stimulates spindles in the isometric condition

Figure 2A-C displays the responses of three additional muscle spindle afferents during the isometric condition, with each afferent originating from a different muscle. All three respond to the locally applied pressure stimulus, with a dynamic component in their responses. Figure 2D shows the mean change in firing rate across all recorded afferents for the different epochs of the 'isometric' condition (see also Figure 2A). Data for this comparison were generated by first normalizing spindle firing rate (z-transform), and then subtracting the mean firing rate observed during the epoch before any pressure was applied i.e., 'baseline' epoch, at the level of single afferents. The recorded afferents were classified as primary ('type Ia') or secondary ('type II'; see Methods for more details), although no systematic differences were subsequently observed as a function of afferent type. Single-sample t-tests indicated that spindle firing rate was significantly different from baseline during all subsequent epochs, with local press inducing stronger responses (F1: t_{13}=3.24, p=0.0064; F2: t_{13}=3.08, p=0.0086; F3: t_{13}=3.97, p=0.0016) and 'release' epochs associated with lower firing rates than baseline (R1: t_{13}=-3.19, p=0.007; R2: t_{13}=-4.03, p=0.0014). A repeated-measures ANOVA of the three press epochs revealed a significant impact of pressure level ($F_{2,26}$=7.4, p=0.003), with Tukey's HSD test indicating significantly higher firing rates at the F3 epoch (vs. F1: p=0.003; vs. F2: p=0.022). Moreover, a dependent-samples t-test indicated significantly lower firing rates in the R2 epoch vs. R1 (t_{13}=2.27, p=0.04). These results suggest that local pressure is an 'adequate' stimulus for muscle spindles in the isometric condition, with significantly higher firing rates for higher press forces (~2N resolution in our study; e.g., Figure 2D), and removal of pressure is associated with lower firing rates than baseline.

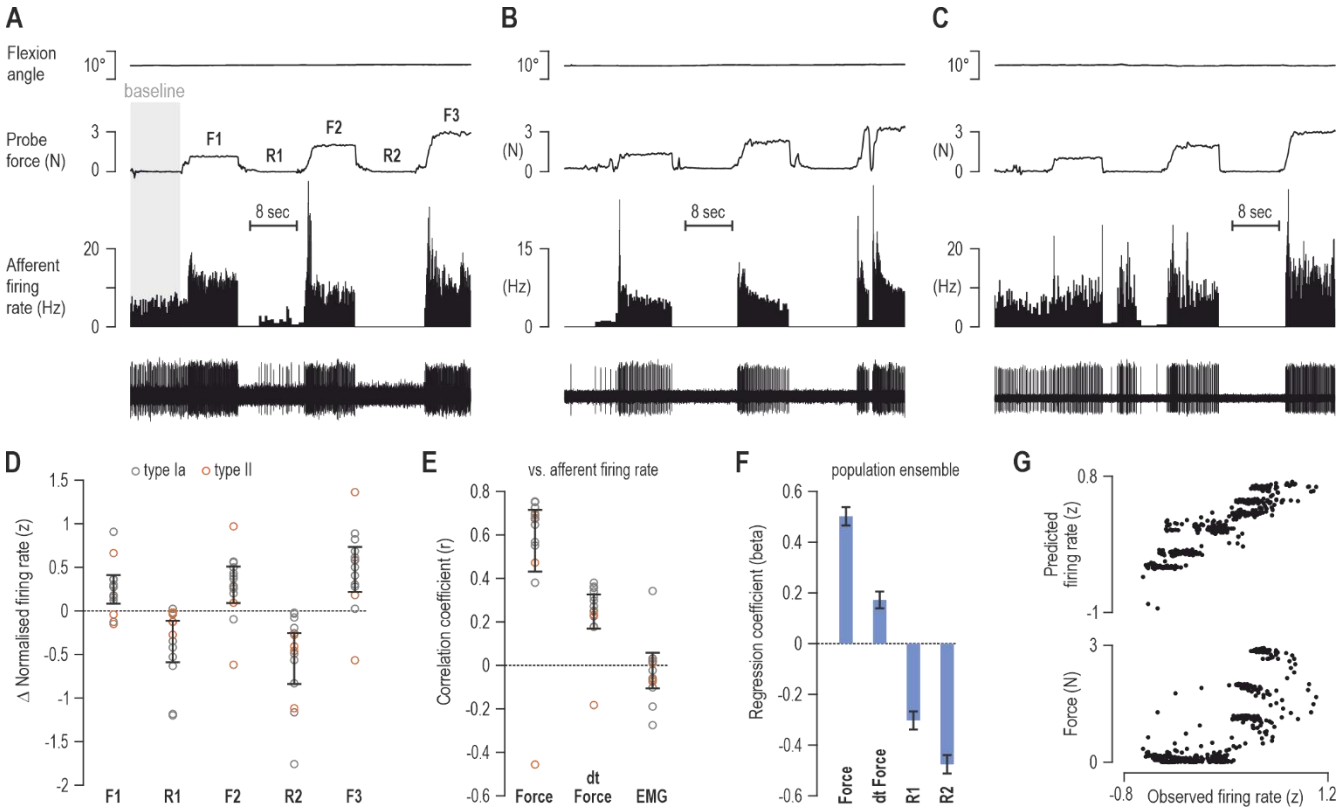

Figure 2. Local muscle pressure is an adequate stimulus for spindle receptors in the isometric condition.

A) A spindle afferent from the common digit extensor muscle displaying vigorous responses to locally applied muscle pressure. For analysis purposes, the latter 8 seconds before application of the first press stimulus was designated as the baseline epoch, and the latter 8 seconds of the subsequent press and release epochs were coded as illustrated (i.e., F1-F3). **B)** As 'a' but representing a spindle afferent from the extensor carpi radialis muscle. **C)** As 'a' but representing a spindle afferent from the extensor carpi ulnaris muscle. **D)** Mean change in

afferent firing rate (from baseline) in the five epochs of the isometric condition, as designated in 'a'. Each circle outline corresponds to a single afferent (N=14). Error bars represent 95% confidence intervals. **E)** Full data sets during the isometric condition (e.g., see 'a'-'c') were down-sampled with a moving average window of 100 ms and correlations performed at the level of individual afferents. Error bars represent 95% confidence intervals, that were Fisher z transformed and then reversed to r. Only one afferent displayed a negative relationship between its firing rate and press force or the first derivative of force ('dt force'; see also Figure S1). **F)** Statistically significant beta (scaleless) regression coefficients following a forward stepwise regression to predict afferent population ensemble responses. Error bars represent 95% confidence intervals. **G)** Above: the regression coefficients in 'f' produced a very good reconstruction of the observed ensemble firing rate. Below: a significant relationship between ensemble firing rate and the ensemble press force signal.

To complement these findings, we also analyzed continuous raw data profiles of single afferents (see e.g., Figure 2A-C), down-sampled with a moving average window of 100 ms. As illustrated in Figure 2E, the firing rate of all but one afferent displayed a positive relationship with press force (95% CI in r [0.71, 0.43]) and with its first derivative (95% CI in r [0.33, 0.17]). Although participants were instructed to remain relaxed during the isometric task, some minor EMG activity was occasionally evident in the spindle-bearing muscle of some participants. The relationship with EMG activity was therefore also examined as a proxy for alpha-gamma co-activation[20], as done previously (see Methods). However, as expected, there was no systematic relationship between EMG and spindle firing across the recorded afferents (95% CI in r [0.06, -0.11]).

The down-sampled profiles were also collapsed across afferents (averaged) to create population ensemble signals for a forward-stepwise regression. Specifically, press force and its first derivative, as well as dummy variables representing the release epochs ('R1' and 'R2') and spindle-bearing muscle EMG were entered as predictors to reconstruct the afferent ensemble responses. A very good reconstruction of ensemble firing rate was achieved (adjusted r^2=0.85, $p<10^{-5}$), with all predictors except EMG exerting a significant impact (force β=0.5, $p<10^{-5}$; force dt β=0.18, $p<10^{-5}$; R1 β=-0.3, $p<10^{-5}$; R2 β=-0.47, $p<10^{-5}$; EMG β=0.02, p=0.19; Figure 2F-G). A strong positive relationship is also evident between the population firing rate and press force, with r=0.75 and $p<10^{-5}$ (Figure 2G, bottom). Performing the above analyses using data down-sampled with a larger moving average window (500 ms) produced virtually identical results (Figure S2). Taken together, our results demonstrate that in isometric conditions spindle neurons are strongly affected by and can encode locally applied muscle pressure.

Muscle pressure enhances spindle responses during stretch

Figure 3A displays the responses of a typical spindle afferent recorded during the 'sinusoidal' condition (see also Figure 1C, right). In this condition, there is no increase in background firing throughout periods of pressure; rather, the afferent responses to muscle stretch (wrist flexion) are stronger during periods of pressure. Figure 3B shows the mean change in afferent firing rates across all recorded afferents for the different epochs of the 'sinusoidal' condition. Data for this comparison was generated as per Figure 2D. Single-sample t-tests confirmed that spindle firing rates were significantly higher than baseline during all epochs where pressure was applied (F1: t_{13}=2.9, p=0.012; F2: t_{13}=2.97, p=0.011; F3: t_{13}=3.83, p=0.002). Moreover, a repeated-measures ANOVA of the three press epochs again produced a significant impact of pressure level ($F_{2,26}$=6.3, p=0.006), with Tukey's HSD test indicating significantly higher firing rates in the F3 epoch vs. F1, with p=0.004. In contrast to the isometric condition, however, single-sample t-tests indicated no systematic difference in firing rate during the 'release' epochs (R1: t_{13}=-0.45, p=0.66; R2: t_{13}=-0.32, p=0.75). As expected, performing single-sample t-tests as above for wrist angle, angular velocity and muscle EMG indicated no significant difference from baseline values in any epoch (all p>0.05).

We also analyzed continuous data profiles of single afferents (see e.g., Figure 3A), down-sampled with a moving average window of 100 ms. However, since it was clear from the raw data profiles that vigorous afferent responses were present only during muscle stretch, these specific analyses were confined to periods of wrist

flexion. As indicated in Figure 3C, the firing of the majority of afferents displayed a positive relationship with flexion angle (95% CI in r [0.63, 0.26]), angular velocity (95% CI in r [0.52, 0.34]), press force (95% CI in r [0.37, 0.14]) and its first derivative (95% CI in r [0.22, 0.14]), but there was no systematic relationship between afferent firing and EMG (95% CI in r [0.1, -0.03]). Population ensemble signals pertaining to the variables named in Figure 3C were used to reconstruct the afferent population firing rate (see Methods for more details). Following a forward stepwise regression, a very good reconstruction of ensemble firing rates was achieved (adjusted r^2=0.95, $p<10^{-5}$) with joint angle, angular velocity and press force emerging as significant predictors (angle β=0.77, $p<10^{-5}$; velocity β=0.7, $p<10^{-5}$; force β=0.31, $p<10^{-5}$). As shown in Figure 3D, the impact of pressure manifested as a positive offset in afferent responses during wrist flexion; there were otherwise no significant differences in r values between spindle firing rate and angle or velocity as a function of press i.e., angle red r (0.61) vs. angle blue r (0.7), p=0.52; velocity red r (0.63) vs. velocity blue r (0.55), p=0.65.

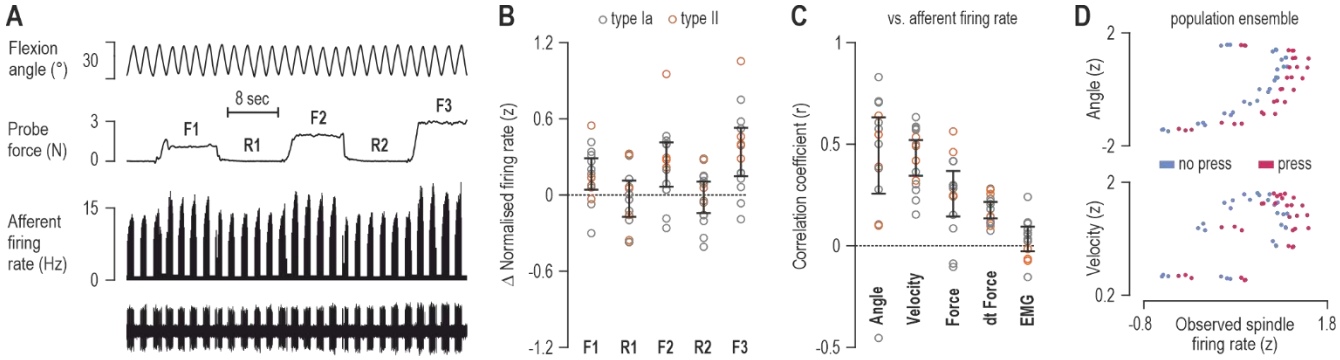

Figure 3. Local muscle pressure enhances spindle responses during stretch.

A) Exemplary responses from a spindle afferent during the sinusoidal condition. Despite the same sinusoidal movement of the hand, higher firing rates are evident in response to muscle stretch (wrist flexion) when local press was applied on the muscle. As per the isometric condition, the latter 8 seconds before application of the first press stimulus was designated as the baseline epoch, and the latter 8 seconds of the subsequent press and release epochs were coded as illustrated (i.e., F1-F3). **B)** Mean change in afferent firing rate (from baseline) in the five epochs of the sinusoidal condition, as designated in 'a'. Each circle outline corresponds to a single afferent (N=14). Error bars represent 95% confidence intervals. **C)** Full data sets in the sinusoidal condition were down-sampled with a moving average window of 100 ms and correlations were performed at the level of individual afferents. Error bars represent 95% confidence intervals that were Fisher z transformed and then reversed to r. **D)** Normalized ensemble population signals during muscle stretch in the sinusoidal condition. Red dots correspond to datapoints during the three press epochs (F1-3) and the blue dots represent the equivalent for the three epochs with no press (i.e., baseline and R1-2). At the population ensemble level (and single afferent level as well; see e.g., 'a'), the impact of muscle pressure on spindles manifested primarily as a positive offset in afferent responses.

Contrast of spindle responses across conditions

Comparing the r^2 values obtained for the relationship between single spindle firing and press force in the isometric condition (Figure 2E) with those obtained for angle (i.e., hand position) and velocity above (Figure 3C) indicated a significantly stronger relationship for the former (Figure 4). These results further reinforce that local pressure should be considered an 'adequate' stimulus for spindles in isometric conditions. Dependent-samples t-tests indicated that press force in the isometric condition was more strongly related to spindle firing than joint angle (t_{13}=2.38, p=0.033) or angular velocity (t_{13}=3.64, p=0.003) during sinusoidal movement. Shapiro-Wilk tests indicated that the distribution of r^2 values relating to press force did not depart from normality (W=0.91, p=0.16), nor did the r^2 values relating to angle (W=0.96, p=0.81) and angular velocity (W=0.93, p=0.35). Last, we recorded from three spindle afferents during active sinusoidal movement, and local pressure again resulted in enhanced spindle responses during stretch (Figure S3).

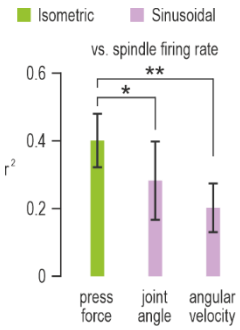

Figure 4. The closest observed relationship is between spindle firing and press force in the isometric condition.

Mean r^2 values across afferents (generated from the r values shown in Figure 2E and Figure 3C) describing the relationship between spindle afferent firing and press force in the isometric condition (green) and the relationship between spindle firing and joint angle/velocity in the sinusoidal condition (pink). Error bars represent 95% confidence intervals. Single star signifies statistical significance at alpha=0.05, and double star signifies statistical significance at alpha=0.01.

DISCUSSION

In the current study, we demonstrate that local muscle pressure is an 'adequate' stimulus for muscle spindles in isometric conditions, and that pressure enhances spindle responses during muscle stretch. Moreover, the relationship between afferent firing and press force in the isometric condition is stronger compared to that between afferent firing and kinematic variables in the sinusoidal condition (Figure 4). That is, individual spindles and their afferents seem better at encoding press force in isometric conditions than joint angle (position) and velocity during muscle stretch. While we used percutaneous press to stimulate spindle receptors in our study with fully-alert humans, evidence in support of the hypothesis that compression of the spindle capsule should occur during muscle contraction have been outlined long ago[16]. Nevertheless, IMP associates naturally with both muscle contraction and percutaneous compression, such as when sitting or leaning on our muscles in everyday life. Our findings therefore serve to redefine naturalistic proprioceptive feedback.

The current study challenges the general belief that the muscle spindles primarily encode static muscle length or stretch[21] and provide consistent information about limb position and velocity[8,9]. Spindle receptor endings are indeed supplied with the stretch-sensitive Piezo2 channel[22], which would argue for a role is sensing muscle stretch. But on the other hand, Piezo2 is the main channel involved in peripheral mechanoreception[23,24], including in skin mechanoreceptors such as the Merkel disk receptor[25] which is known to encode pressure and texture[8,26]. In other words, the structure of the (encapsulated) sensory organs can be decisive in terms of shaping their afferent signals. Moreover, spindles are unique peripheral sensory organs in that their output can be controlled independently by the nervous system itself, via gamma motor (fusimotor) neurons[27,28], which comprise an astonishing ~30% of all lower motor neurons[29,30]. Over the years, several hypotheses have been put forward regarding the role of fusimotor control, including the maintenance of stretch sensitivity during skeletal muscle contraction, thought enabled by co-activation of alpha motor and fusimotor neurons[20]. A recent proposal[31] views fusimotor signals as representing an intermediate coordinate transformation that allows spindle organs to receive converging information from other sensory modalities (e.g., from vision and skin). Fusimotor input therefore allows spindle organs to function as controllable signal processing 'devices' that can produce flexible coordinate representations, and whose overarching role is to facilitate sensorimotor performance, including in terms of postural stability. Such a role is compatible with established findings and supported by recent studies with naturalistically active humans[32-35]. Fusimotor input is thought to allow dynamic control over muscle feedback according to task characteristics and even different goals within a task[34], rather

than exclusively promote the encoding of veridical limb position and velocity. Nevertheless, the current study concentrated on examining the ability of the spindle organ to encode physical stimuli, a crucial aspect of spindle function upon which fusimotor control can potentially act.

Or findings demonstrate that spindles encode percutaneous press force especially well during the isometric task. The spindle response to the pressure stimulus in the isometric condition involved a positive offset in firing and was often accompanied with an additional, relatively minor, dynamic component (i.e., response to dt force; see Figure 2E). The positive offset in afferent firing with pressure could primarily reflect stimulation of nuclear chain fibers[17,18,36], as initially proposed by Bridgman and Eldred[16] (see also Introduction section). The dynamic component could possibly reflect stimulation beyond nuclear chain fibers e.g., some nuclear bag fibers also terminate near the polar ends of the spindle capsule[37]. Be that as it may, the afferent response profiles during press in the isometric condition look very similar to those previously demonstrated during isometric contractions[38], with spindle responses in those cases believed to arise due to co-activation of alpha and gamma motor neurons[20]. Because muscle contraction is accompanied by increases in IMP[1-3], it is quite possible that spindle responses during isometric contraction largely result from increased levels of IMP (i.e., compression of the spindle capsule) rather than arise due to neural control of spindles.

The ability of spindles to encode local muscle pressure urges a re-evaluation of the role of proprioceptive muscle feedback in sensorimotor function[9,31,39] (especially in the context of postural maintenance) and in various neuromuscular conditions[40], including the case of exercise-induced muscle cramps[41,42]. Access to sensory feedback concerning muscle pressure gradients could empower more robust sensorimotor control, such as through better balancing of motor unit recruitment[16], and direct incorporation the muscle's fluidic behavior in reflex responses and more global muscle activation strategies[7]. Indeed, it has recently been suggested that proprioceptive feedback does contribute to the maintenance of spinal realignment[14]. Moreover, it has been repeatedly suggested that muscle spindles may contribute to the sense of effort, heaviness or force[43-47]. While it has been unclear how muscle spindles may provide a continuously reliable muscle force signal[47,48], it has been speculated that neural control based on alpha-gamma co-activation may aid in this purpose[44]. We suggest that, via compression of the spindle capsule, muscle spindles can encode press force and IMP in particular, with the latter known to be a more reliable index of muscle force than muscle electrical activity[4,5].

Limitations

One clear limitation in this study involves using the press force associated with the percutaneous compression of muscle as a proxy for the IMP exerted on the recoded spindle organ. While our minimally invasive *in vivo* study allowed us to document and characterize naturalistic proprioceptive feedback in humans, more invasive animal studies can elucidate further the impact of IMP on spindle organ compression in healthy and diseased muscle. For example, this can be achieved by using catheters to monitor local IMP during simultaneous recording of sensory afferent feedback or via direct intramuscular compression of spindle capsules in more reduced preparations.

STAR METHODS

REAGENT or RESOURCE	SOURCE	IDENTIFIER
Deposited data		
Analyzed data	This paper; Mendeley Data	DOI: 10.17632/549wt8drc7.1
Software and algorithms		
MATLAB	MathWorks, Natick	https://se.mathworks.com/products/matlab.html
Statistica	StatSoft Inc	https://www.statistica.com/en/

RESOURCE AVAILABILITY

Lead contact

Reasonable requests for further information and data resources should be directed to and will be fulfilled by the lead contact, Michael Dimitriou (michael.dimitriou@umu.se).

Materials availability

This study did not involve any newly generated unique material.

Data and code availability

- Analyzed data sets have been deposited at Mendeley and are publicly available as of the date of publication. Accession numbers are listed in the key resources table. Multiple raw data profiles are displayed in graphical form throughout the paper (e.g., Figure 1-3; S1; S3).
- Any additional information required to analyze the data reported in this paper is available from the lead contact upon reasonable request.

PARTICIPANT DETAILS

Eight neurologically healthy adult human volunteers participated in the current study (mean age 24.5 years ± 4.7 standard deviations; half self-identified as female and half as male). The participants provided written informed consent prior to participation, in accordance with the Declaration of Helsinki, and were financially compensated. No statistical method was used to determine sample size, but the number of participants (and single afferents) in the current study is similar or exceeds the number used in equivalent studies (see e.g.,[34,49]). Our study was conducted as part of a research programme approved by the Umeå Regional Ethics Committee.

METHOD DETAILS

Muscle afferent recordings

Microneurography (MNG) was used to record single spindle afferent activity in the radial nerve of the right arm[50,51,], as previously done in our lab[32-34]. Afferent recordings were obtained from either the radial wrist extensor (extensor carpi radialis), the ulna wrist extensor (extensor carpi ulnaris) or the common digit extensor (extensor digitorum communis). The recorded action potentials were identified as originating from primary or secondary muscle spindles (vs. e.g., Golgi tendon organ or skin receptors) according to standard procedures described in detail elsewhere[52-54]. In short, these procedures include examining the afferent responses to ramp and hold stretches of the relaxed spindle-bearing muscle, the response to taps on the muscle (vs. skin of the hand) and assessing the variability in background firing rate[55]. In total, 14 muscle spindle afferents were recorded

(10 'type Ia' and 4 'type II'). Each participant contributed with at least one afferent recording. The number of afferents recorded here is similar or exceeds the number of afferents recorded in previous MNG studies with human participants[33,34,52,56].

Electromyography (EMG)

Custom-made surface EMG electrodes, with a diameter of 2 mm and an internal distance of 12 mm were attached to three forearm muscles. Specifically, recordings were made from the extensor carpi ulnaris, extensor carpi radialis and extensor digitorum communis. Electrode placement was selected using a hand-held stimulator probe and isometric contraction/relaxation maneuvers. Prior to placement the EMG electrodes were coated with conductive gel, and then attached with double-sided tape. A ground electrode was placed on the lateral epicondyle of the humerus bone.

Experimental set-up and design

Participants sat on an adjustable dental chair with their right arm resting on a padded cushion. The chair was tilted backward and adjusted to fit the participant's stature and shape. The forearm was secured in place using a padded wooden vise proximal to the wrist, and this allowed the hand to move freely while the arm was stabilized to prevent displacement of the MNG electrode. Visual feedback was provided by a monitor placed opposite the participant at approximately eye-level (see Figure 1A). Two vertical targets (26.5 cm long and 0.8 cm wide, located 8.5 cm from the origin) were continuously displayed on the monitor, and hand position was represented by a vertical cursor/line (25.5 cm long and 0.3 cm wide). Hand kinematics were recorded using a FASTRAK® sensor attached to the dorsal surface of the hand with double-sided tape and fixated with surgical tape. Movement of the semi-pronated hand about the wrist in the flexion-extension dimension controlled the 1D cursor position along the horizontal axis (i.e., between the visual targets).

The current study involved two experimental conditions (Figure 1B). In the first condition ('isometric'), the participant's hand was relaxed and immobile, resting on a cushion in a lightly flexed position at the wrist. Note that the label 'isometric' refers here to the lack of any externally perceptible movement of the participant's hand. Before the onset of the second 'sinusoidal' condition, the experimenter first grasped the lightly fisted hand of the participant and then moved the participant's hand in the initial position. In the initial position, the participant's hand (i.e., third metacarpal joint) was aligned with the longitudinal axis of the forearm (i.e., zero flexion/extension and ulna/radial deviation), and this corresponded to the cursor being in the center of the screen, between the two visual targets. The sinusoidal task then followed, which involved the experimenter moving the participant's lightly fisted hand rhythmically about the wrist in the flexion-extension dimension at a 0.5 Hz pace. The speed of hand movements was guided by a metronome and movement amplitude was guided by the visual targets i.e., the experimenter moved the cursor so that it alternated in reaching each of the two targets. One three occasions, single afferent recordings were made while the participants performed the sinusoidal movements actively, also using the metronome and visual targets to control the pace and amplitude of their movements (Figure S3). Throughout, a rotation of one degree at the wrist corresponded to a 0.7 cm movement of the cursor along the horizontal axis of the monitor. Because the distance between the center of the screen and the center of a target was 8.5 cm, a wrist rotation of ~12 degrees was required for reaching the middle of each target from the initial position.

During each experimental condition, we applied pressure percutaneously on one of three major extensor muscles of the forearm using a hand-held probe. Specifically, the press force on the muscle was applied using a probe with an embedded six-axis force/torque transducer (Nano F/T transducer; ATI Industrial Automation), and

a flat circular contact area of 5mm diameter. As indicated by the schematic at the bottom of Figure 1B, after an idle period of 10 seconds (corresponding to the 'baseline' epoch; see e.g., Figure 2A) three sequential target levels of press force (1, 2, and 3N) were applied in each experimental condition. The onset and offset time for applying a pressure stimulus, as well as the magnitude of the stimulus for any press, was indicated to a second experimenter (other than the one moving the hand in the sinusoidal condition) by a message shown on a second monitor. The second monitor was placed across the second experimenter, and outside the visual field of the participant. Each of the 'press' message on the second monitor lasted for 10 seconds, as did the 'release' messages. Some minor discrepancy was to be expected between the duration of the visual messages and that of the actual press epochs, due to the reaction time of the second experimenter. However, in addition to performing complementary analyses with continuous data profiles (e.g., Figure 2E-G), analyses were confined to the latter 8 seconds of each epoch where necessary (e.g., Figure 2D), as the experimenter's reaction time never exceeded 2 seconds. Concerning the magnitude of the applied press force, the experimenter received continuous real-time feedback in the form of a horizontal flat bar moving vertically along a background scale shown on the second monitor, with increases in force corresponding to movement of the bar towards the top of the scale.

Before inserting the MNG electrode, participants were familiarized with the two experimental conditions, including experiencing a dry run of the sinusoidal condition and performing the sinusoidal movement themselves. The participants were asked to remain relaxed and passive during the isometric and sinusoidal conditions. On three occasions where the afferent recording seemed particularly stable as the end of the passive sinusoidal movement (hence likely not to be lost during active movement), the participants performed the sinusoidal movement actively under pressure and release for comparison (Figure S3).

QUANTIFICATION AND STATISTICAL ANALYSIS

Data sampling and pre-processing

Data sampling was performed using SC/ZOOM™. With SC/ZOOM™ single action potentials were identified semi-automatically under visual control. The simultaneously recorded EMG channels were high-pass filtered with a 30 Hz cutoff and then root-mean-square processed with a symmetrical +-3.0 ms window. They were digitally sampled at 4800 Hz. All data used for analyses, including EMG, were extracted from SC/ZOOM™ at a 1000 Hz rate. To facilitate comparison of EMG and afferent recordings across muscles and participants, the raw data were normalized by z-transformation using a procedure that has been described elsewhere[33,35,52]. In brief, for each individual afferent/participant, and each data variable, a grand mean and grand standard deviation was generated across all continuous datapoints. The z-transformed data was obtained by subtracting the grand mean from the measured value and dividing the difference by the grand standard deviation. To generate the down-sampled data that was entered into correlations and regression analyses, a moving average window of 100 ms was used on the recorded raw data profile of each afferent (e.g., Figure 2A-C & 3A). To generate the population ensemble signals of the isometric condition, the down-sampled profiles were collapsed (averaged) across afferents (N=14). All afferents were used in this procedure, including the one with a net negative relationship to muscle pressure (Figure S1). Note that in one afferent profile (out of 14) the EMG signals alone were lost due to an acute battery issue with the recording equipment and therefore treated as missing data. Using a larger down-sampling window produced equivalent correlation and regression results (Figure S2). To generate the population ensemble signals pertaining to the sinusoidal condition (i.e., Figure 3D), a different approach was taken. For each single afferent separately, the raw data for each movement cycle was identified and re-sampled to 2 sec (corresponding to the target pace of movement: 0.5 Hz), and then collapsed (averaged) across the number of repetitions for each epoch (i.e., 6 epochs: baseline and F1-F3 as designated in Figure 3A). The data for each of

the 6 averaged cycles per afferent where then down-sampled with a moving average window of 100ms (resulting in 20 data points per cycle), and finally averaged data cycles were collapsed across afferents to create the population ensemble signals, totaling 120 data points for each variable (6 epochs x 20 points each cycle; Figure 3D). Throughout, data pre-processing was performed using Matlab® (R2019a, MathWorks, Natick, MA, USA).

Statistical analyses

To assess the impact of press force on spindle afferent firing, all statistical analyses were two-tailed, where applicable. These involved single-sample t-tests to assess significant deviation in firing rate from baseline levels, as well as repeated-measures ANOVA to assess the effect of pressure level, along with Tukey's posthoc analyses and dependent-samples t-tests to compare firing rates across epochs (Figure 2D & 3B). Single-sample t-tests were also employed to confirm the lack of significant deviation in wrist angle, velocity and EMG from baseline as a function of task epoch. Pearson's correlation coefficients ('r') were calculated to assess the relationship between firing rate and various independent variables, both at the single afferent level and at the population level (Figure 2E,G & 3C). Dependent sample t-tests were used to contrast the strength of relationship between firing rate and press force in the isometric condition and that between firing rate and kinematic variables in the sinusoidal condition (Figure 4). Forward-stepwise regressions were used for identifying the significant predictors of afferent ensemble firing rate, using z-transformed data (Figure 2G & 3D). Beta coefficients are reported which represent the standard deviation change in the dependent variable (here afferent firing rate) for 1 standard deviation change in the predictor variable. To assess data normality, Shapiro-Wilks test was used for sample sizes <50 data points, otherwise the Lilliefors test was used. Throughout, the level of statistical significance was 0.05. Correlation analyses at the level of single afferents were performed using Matlab® (R2019a, MathWorks, Natick, MA, USA), whereas all other statistical analyses were performed using STATISTICA® (StatSoft Inc, USA).

ACKNOWLEDGMENTS

The authors would like to thank Carola Hjältén and Anders Bäckström for their technical support. This work was supported by grants awarded to M.D. by the Medical Faculty of Umeå University strategic grant (2.1.6-56-23), and the Swedish Research Council (2020-02140). The funders had no role in study design, data collection, analysis, decision to publish, or manuscript preparation.

Author contributions

M.D. conceived and funded the study; M.D. collected the data; M.D. and F.T. analyzed the data; M.D. and F.T. interpreted the data; M.D. and F.T. wrote the paper; M.D. supervised the study.

Declaration of interests

The authors declare no competing interests.

Inclusion and diversity statement

We support inclusive, diverse, and equitable conduct in research.

REFERENCES

1. Sejersted, O.M., and Hargens, A.R. (1995). Intramuscular pressures for monitoring different tasks and muscle conditions. Adv Exp Med Biol *384*, 339-350. 10.1007/978-1-4899-1016-5_27.
2. Davis, J., Kaufman, K.R., and Lieber, R.L. (2003). Correlation between active and passive isometric force and intramuscular pressure in the isolated rabbit tibialis anterior muscle. J Biomech *36*, 505-512. 10.1016/s0021-9290(02)00430-x.
3. Sejersted, O.M., Hargens, A.R., Kardel, K.R., Blom, P., Jensen, O., and Hermansen, L. (1984). Intramuscular fluid pressure during isometric contraction of human skeletal muscle. J Appl Physiol Respir Environ Exerc Physiol *56*, 287-295. 10.1152/jappl.1984.56.2.287.
4. Aratow, M., Ballard, R.E., Crenshaw, A.G., Styf, J., Watenpaugh, D.E., Kahan, N.J., and Hargens, A.R. (1993). Intramuscular pressure and electromyography as indexes of force during isokinetic exercise. J Appl Physiol (1985) *74*, 2634-2640. 10.1152/jappl.1993.74.6.2634.
5. Sjøgaard, G., Jensen, B.R., Hargens, A.R., and Søgaard, K. (2004). Intramuscular pressure and EMG relate during static contractions but dissociate with movement and fatigue. J Appl Physiol (1985) *96*, 1522-1529; discussion. 10.1152/japplphysiol.00687.2003.
6. Sleboda, D.A., and Roberts, T.J. (2020). Internal fluid pressure influences muscle contractile force. Proc Natl Acad Sci U S A *117*, 1772-1778. 10.1073/pnas.1914433117.
7. El Bojairami, I., and Driscoll, M. (2022). Formulation and exploration of novel, intramuscular pressure based, muscle activation strategies in a spine model. Comput Biol Med *146*, 105646. 10.1016/j.compbiomed.2022.105646.
8. Gardner, E.P. (2021). Receptors of the somatosensory system. In Principles of Neural Science, E.R. Kandel, J.D. Koester, S.H. Mack, and S.A. Siegelbaum, eds. (McGraw Hill), pp. 415.
9. Prochazka, A. (1996). Proprioceptive feedback and movement regulation. In Exercise: Regulation and integration of multiple systems, L. Rowell, and J.T. Shepherd, eds. (American Physiological Society), pp. 89-127.
10. Proske, U., and Gandevia, S.C. (2012). The proprioceptive senses: their roles in signaling body shape, body position and movement, and muscle force. Physiol Rev *92*, 1651-1697.
11. Matthews, P.B.C. (1972). (Edward Arnold Publishers Ltd).
12. Houk, J.C. (1976). An assessment of stretch reflex function. Prog Brain Res *44*, 303-314.
13. Hwang, E.J., and Shadmehr, R. (2005). Internal models of limb dynamics and the encoding of limb state. J. Neural Eng. *2*, S266-S278.
14. Blecher, R., Krief, S., Galili, T., Biton, I.E., Stern, T., Assaraf, E., Levanon, D., Appel, E., Anekstein, Y., Agar, G., et al. (2017). The Proprioceptive System Masterminds Spinal Alignment: Insight into the Mechanism of Scoliosis. Developmental cell *42*, 388-399.e383. 10.1016/j.devcel.2017.07.022.
15. Blecher, R., Krief, S., Galili, T., Assaraf, E., Stern, T., Anekstein, Y., Agar, G., and Zelzer, E. (2017). The Proprioceptive System Regulates Morphologic Restoration of Fractured Bones. Cell reports *20*, 1775-1783. 10.1016/j.celrep.2017.07.073.
16. Bridgman, C.F., and Eldred, E. (1964). Hypothesis for a pressure-sensitive mechanism in muscle spindles. Science *143*, 481-482. 10.1126/science.143.3605.481.
17. Banks, R.W., Harker, D.W., and Stacey, M.J. (1977). A study of mammalian intrafusal muscle fibres using a combined histochemical and ultrastructural technique. J Anat *123*, 783-796.
18. Boyd, I.A. (1958). The innervation of mammalian neuromuscular spindles. J Physiol *140*, 14-15p.
19. Boyd, I.A. (1980). The isolated mammalian muscle spindle. Trends in Neurosciences *3*, 258-265. https://doi.org/10.1016/0166-2236(80)90096-X.
20. Vallbo, A.B. (1970). Discharge patterns in human muscle spindle afferents during isometric voluntary contractions. Acta Physiol Scand *80*, 552-566.
21. Edin, B.B., and Vallbo, A.B. (1990). Dynamic response of human muscle spindle afferents to stretch. J Neurophysiol *63*, 1297-1306.
22. Woo, S.H., Lukacs, V., de Nooij, J.C., Zaytseva, D., Criddle, C.R., Francisco, A., Jessell, T.M., Wilkinson, K.A., and Patapoutian, A. (2015). Piezo2 is the principal mechanotransduction channel for proprioception. Nat Neurosci *18*, 1756-1762. 10.1038/nn.4162.
23. Anderson, E.O., Schneider, E.R., and Bagriantsev, S.N. (2017). Piezo2 in Cutaneous and Proprioceptive Mechanotransduction in Vertebrates. Curr Top Membr *79*, 197-217. 10.1016/bs.ctm.2016.11.002.
24. Chesler, A.T., Szczot, M., Bharucha-Goebel, D., Čeko, M., Donkervoort, S., Laubacher, C., Hayes, L.H., Alter, K., Zampieri, C., Stanley, C., et al. (2016). The Role of PIEZO2 in Human Mechanosensation. The New England journal of medicine *375*, 1355-1364. 10.1056/NEJMoa1602812.
25. Ikeda, R., Cha, M., Ling, J., Jia, Z., Coyle, D., and Gu, Jianguo G. (2014). Merkel Cells Transduce and Encode Tactile Stimuli to Drive Aβ-Afferent Impulses. Cell *157*, 664-675. https://doi.org/10.1016/j.cell.2014.02.026.
26. Westling, G., and Johansson, R.S. (1987). Responses in glabrous skin mechanoreceptors during precision grip in humans. Exp Brain Res *66*, 128-140. 10.1007/bf00236209.
27. Barker, D., and Chin, N.K. (1961). Efferent Innervation of Mammalian Muscle-spindles. Nature *190*, 461-462. 10.1038/190461a0.

28. Crowe, A., and Matthews, P.B. (1964). Further Studies of Static and Dynamic Fusimotor Fibres. J Physiol *174*, 132-151. 10.1113/jphysiol.1964.sp007477.
29. Burke, R.E., Strick, P.L., Kanda, K., Kim, C.C., and Walmsley, B. (1977). Anatomy of medial gastrocnemius and soleus motor nuclei in cat spinal cord. J Neurophysiol *40*, 667-680. 10.1152/jn.1977.40.3.667.
30. Kuffler, S.W., Hunt, C.C., and Quilliam, J.P. (1951). Function of medullated small-nerve fibers in mammalian ventral roots; efferent muscle spindle innervation. J Neurophysiol *14*, 29-54. 10.1152/jn.1951.14.1.29.
31. Dimitriou, M. (2022). Human muscle spindles are wired to function as controllable signal-processing devices. eLife *11*, e78091. 10.7554/eLife.78091.
32. Dimitriou, M. (2014). Human Muscle Spindle Sensitivity Reflects the Balance of Activity between Antagonistic Muscles. J Neurosci *34*, 13644-13655. 10.1523/JNEUROSCI.2611-14.2014.
33. Dimitriou, M. (2016). Enhanced Muscle Afferent Signals during Motor Learning in Humans. Curr Biol *26*, 1062-1068. 10.1016/j.cub.2016.02.030.
34. Papaioannou, S., and Dimitriou, M. (2021). Goal-dependent tuning of muscle spindle receptors during movement preparation. Sci Adv *7*. 10.1126/sciadv.abe0401.
35. Dimitriou, M. (2018). Task-dependent modulation of spinal and transcortical stretch reflexes linked to motor learning rate. Behavioral neuroscience *132*, 194-209. 10.1037/bne0000241.
36. Barker, D., Banks, R.W., Harker, D.W., Milburn, A., and Stacey, M.J. (1976). Studies of the histochemistry, ultrastructure, motor innervation, and regeneration of mammalian intrafusal muscle fibres. Prog Brain Res *44*, 67-88. 10.1016/s0079-6123(08)60724-4.
37. Boyd, I.A. (1962). The structure and innervation of the nuclear bag muscle fibre system and the nuclear chain muscle fibre system in mammalian muscle spindles. Philosophical Transactions of the Royal Society of London. Series B, Biological Sciences *245*, 81-136. doi:10.1098/rstb.1962.0007.
38. Edin, B.B., and Vallbo, A.B. (1990). Muscle afferent responses to isometric contractions and relaxations in humans. J Neurophysiol *63*, 1307-1313.
39. Alessandro Marin, V., Axel, B., Alberto, C., Chris, V., Lee, M., and Alexander, M. (2023). Task-driven neural network models predict neural dynamics of proprioception. bioRxiv, 2023.2006.2015.545147. 10.1101/2023.06.15.545147.
40. Kröger, S., and Watkins, B. (2021). Muscle spindle function in healthy and diseased muscle. Skeletal Muscle *11*, 3. 10.1186/s13395-020-00258-x.
41. Minetto, M.A., Holobar, A., Botter, A., Ravenni, R., and Farina, D. (2011). Mechanisms of cramp contractions: peripheral or central generation? J Physiol *589*, 5759-5773. 10.1113/jphysiol.2011.212332.
42. Maughan, R.J., and Shirreffs, S.M. (2019). Muscle Cramping During Exercise: Causes, Solutions, and Questions Remaining. Sports medicine (Auckland, N.Z.) *49*, 115-124. 10.1007/s40279-019-01162-1.
43. Luu, B.L., Day, B.L., Cole, J.D., and Fitzpatrick, R.C. (2011). The fusimotor and reafferent origin of the sense of force and weight. J. Physiol. *589*, 3135-3147.
44. Monjo, F., and Allen, T. (2023). What if muscle spindles were also involved in the sense of effort? The Journal of Physiology *601*, 3453-3459. https://doi.org/10.1113/JP284376.
45. Brooks, J., Allen, T.J., and Proske, U. (2013). The senses of force and heaviness at the human elbow joint. Exp Brain Res *226*, 617-629. 10.1007/s00221-013-3476-6.
46. Proske, U. (2005). What is the role of muscle receptors in proprioception? Muscle Nerve *31*, 780-787.
47. Proske, U., and Allen, T. (2019). The neural basis of the senses of effort, force and heaviness. Exp Brain Res. 10.1007/s00221-018-5460-7.
48. Blum, K.P., Lamotte D'Incamps, B., Zytnicki, D., and Ting, L.H. (2017). Force encoding in muscle spindles during stretch of passive muscle. PLoS computational biology *13*, e1005767. 10.1371/journal.pcbi.1005767.
49. Ribot-Ciscar, E., Rossi-Durand, C., and Roll, J.P. (2000). Increased muscle spindle sensitivity to movement during reinforcement manoeuvres in relaxed human subjects. J Physiol *523 Pt 1*, 271-282. 10.1111/j.1469-7793.2000.t01-1-00271.x.
50. Vallbo, A.B., and Hagbarth, K.E. (1968). Mechnoreceptor activity recorded from human peripheral nerves. Electroencephalogr Clin Neurophysiol *25*, 407.
51. Vallbo, A.B., and Hagbarth, K.E. (1967). Impulses recorded with micro-electrodes in human muscle nerves during stimulation of mechanoreceptors and voluntary contractions. Electroencephalography and clinical neurophysiology *23*, 392.
52. Dimitriou, M. (2014). Human muscle spindle sensitivity reflects the balance of activity between antagonistic muscles. J Neurosci *34*, 13644-13655. 10.1523/JNEUROSCI.2611-14.2014.
53. Dimitriou, M., and Edin, B.B. (2008). Discharges in human muscle spindle afferents during a key-pressing task. J Physiol *586*, 5455-5470. 10.1113/jphysiol.2008.160036.
54. Dimitriou, M., and Edin, B.B. (2008). Discharges in Human Muscle Receptor Afferents during Block Grasping. The Journal of Neuroscience *28*, 12632-12642. 10.1523/jneurosci.3357-08.2008.
55. Nordh, E., Hulliger, M., and Vallbo, A.B. (1983). The variability of inter-spike intervals of human spindle afferents in relaxed muscles. Brain Res *271*, 89-99. 10.1016/0006-8993(83)91367-7.
56. Vallbo, A.B., and al-Falahe, N.A. (1990). Human muscle spindle response in a motor learning task. J Physiol *421*, 553-568. 10.1113/jphysiol.1990.sp017961.

SUPPEMENTARY FIGURES

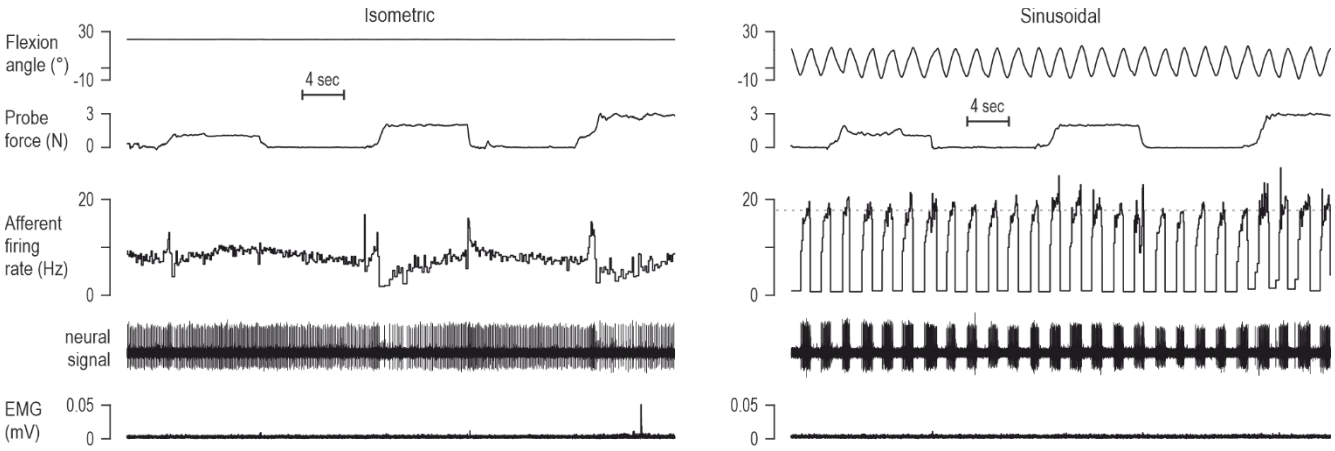

Figure S1. The only recorded spindle afferent with a net negative relationship to muscle pressure in the isometric condition.

Left: responses of the only recorded spindle afferent that displayed a negative overall relationship with press force in the isometric condition. Note, however, the brief increase in firing rate at the onset of each of the three press stimuli (i.e., the afferent did respond to brief taps at the location of the muscle where the probe subsequently pressed). Right: during the sinusoidal condition, the same afferent responded consistently to wrist flexion (i.e., muscle stretch) with some minor increase in firing rate during the early movement cycles when the 2N and 3N press force was applied.

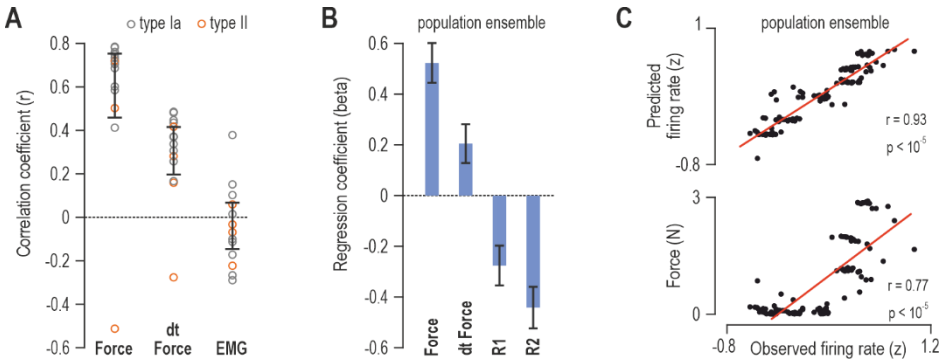

Figure S2. A larger down-sampling window produces qualitatively the same results.

A-C) As Figure 2E-F but using a larger moving average time window (500 ms) to down-sample the continuous data. Qualitatively the same results were obtained.

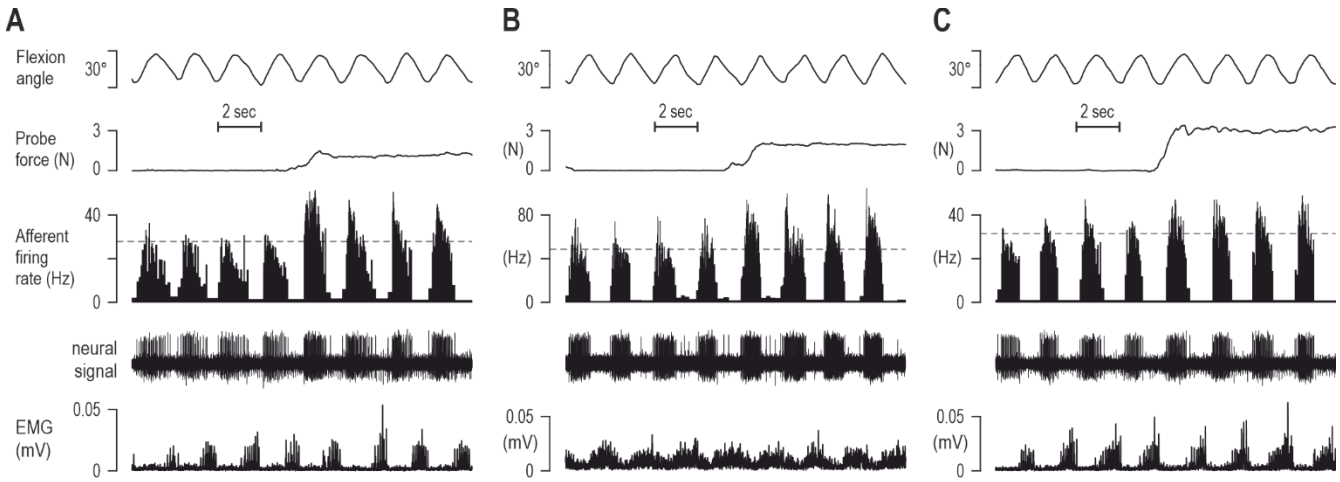

Figure S3. Local muscle pressure enhances spindle responses to stretch in active movement.

A-C) Responses from three separate spindle afferents during active movement of the hand, as per the sinusoidal condition. Despite very similar movement of the hand in each case, higher firing rates are evident in response to muscle stretch (wrist flexion) when local press was applied on the muscle, especially for the afferents in 'A' and 'B'.